

## A Transformed Coordinates Shallow Water Model for the Head of the Bay of Bengal Using Boundary-Fitted Curvilinear Grids

Farzana Hussain\*

*Department of Mathematics, Shahjalal University of Science & Technology, Sylhet,  
Bangladesh.*

*Received 13 June 2012; Accepted (in revised version) 21 February 2013*

*Available online 28 February 2013*

---

**Abstract.** The Bay of Bengal is surrounded by coastline except to the south, where there is open sea. The coastline bends most sharply along the coast of Bangladesh, and there are many small and large islands in the offshore region there. In order to incorporate the island boundaries and the curved coastline properly, in any numerical scheme it is often necessary to consider a very fine grid resolution along the coastal belts whereas this is unnecessary away from the coasts. However, a very fine resolution involves more memory and more CPU time in the numerical solution process, and invites numerical instability. On the other hand, boundary-fitted curvilinear grids in hydrodynamic models for coastal seas, bays and estuaries not only fit to the coastline but also render the finite difference schemes simpler and more accurate. In this article, the boundary-fitted curvilinear grids for the model represent the complete boundary of the area considered by four curves defined by four functions, and the four boundaries of two of the larger islands are then represented approximately by two general functions. An appropriate independent coordinate transformation maps the curvilinear physical area to a square domain, and each island boundary is transformed to a rectangle within this square domain. The vertically integrated shallow water equations are transformed to the new space domain, and solved by a regular explicit finite difference scheme. The model is applied to compute the water levels due to astronomical tides, and also the water levels due to surges associated with tropical storms that hit the coast of Bangladesh.

**AMS subject classifications:** 35F30, 37M05, 65N06, 65N22, 65N50

**Key words:** Tropical storms, surge, tide generation, shallow water equations, boundary-fitted grids, Bay of Bengal.

---

### 1. Introduction

Tropical storms pose the most destructive natural disasters for the coastal region of Bangladesh, and the associated surges are usually more dangerous than the storms themselves. Sometimes a surge may rise from 9 to 12 meters as it rushes towards the land [12],

---

\*Corresponding author. *Email address:* farzanahn@live.com (F. Hussain)

where it causes very severe damage to life and property. There are various factors responsible for the large surge levels along the coast of Bangladesh — such as shallowness of water, off-shore islands, the bending of the coastline, oceanic bathymetry, low lying islands, huge discharge through the rivers, etc.. Moreover, the tidal range (the difference between the high and low tide) is large at the head Bay of Bengal, and if a storm approaches the coast at the time of a high tide the devastation is much worse.

Many analyses have been done for the coast of Bangladesh since 1972, after the major devastation from the November 1970 storm [1–13]. They are based on vertically integrated two-dimensional models and fall into two main categories — viz. stair step models and partially boundary-fitted transformed coordinate models. The coastal and island boundaries are approximated along the nearest finite difference gridlines of the numerical scheme in a stair step model, so its accuracy depends on the grid size. If the grid size is not small, the representation of the coastal boundaries is not accurate. In a boundary-fitted transformed coordinate model, the curvilinear boundaries are transformed into straight lines such that regular finite difference methods can be used in the transformed domain. The pioneering works of Das [1] and Flierl & Robinson [2] were linear stair step models where the friction coefficient was neglected. The stair step model of Das *et al.* [3] was an extension of Das [1], to simulate tidal and surge interactions along the east coast of India and the coast of Bangladesh. The nonlinear stair step model of Johns & Ali [4] included the major rivers and islands, in simulating tidal and surge interaction along the coast of Bangladesh. This model was also used to verify the effect of cyclone tracks and islands on surge levels, and to compute the extent of inland flooding. However, a very fine resolution could not be considered, so the representation of the coastal boundaries in these models was not accurate. To more accurately account for bending coastlines and offshore islands, Roy [12] developed a fine mesh numerical scheme for the Meghna estuary nested into a coarse mesh scheme extending up to 15°N latitude. In the fine mesh component, all of the major islands were incorporated through a proper stair step representation. This model is similar to that of Johns *et al.* [9] for the East Coast of India and the coast of Bangladesh. Johns *et al.* [7] first used partially boundary-fitted curvilinear grids in a transformed coordinate model for the east coast of India to simulate the surge generated by the Andra Cyclone of 1977. In their scheme, the east coast of India and the western open sea boundary were considered as curves represented by two functions, and the north and south open sea boundaries were represented by straight lines. The spatial coordinate transformation they applied mapped the physical domain into a rectangular one. Dube *et al.* [5] represented the natural shoreline of the Bangladesh coast by a curvilinear boundary and used boundary-fitted curvilinear grids. A transformation similar to that of Johns *et al.* [7] was applied in order to make the computational domain rectangular, where an explicit finite difference scheme was used to integrate the shallow water equations. Roy [11] used the model of Dube *et al.* [5] to test the sensitivity of the surge level due to various meteorological and oceanographic factors along the Bangladesh coast. Dube *et al.* [6], Johns *et al.* [8,9] and Sinha *et al.* [10] represented coastlines by curvilinear boundaries and also invoked coordinate transformations, but did not incorporate any offshore islands. The main difficulty in incorporating the islands was that the whereabouts of their boundaries

were undetectable in the transformed domain. Actually, the Bay of Bengal is surrounded by coastline on all sides except in the south, where there is open sea. Moreover, the coastline is curvilinear and the bending is very high along the coast of Bangladesh, and there are many small and large offshore islands. Roy [13] developed a mathematical technique to incorporate some islands of special shape, with boundaries approximated along boundary-fitted gridlines. The two curved boundaries of the domain were defined by two functions, and a general function was consequently defined to represent the boundary-fitted gridlines. The two opposite curved boundaries of each island were then represented approximately by a general function based on the two functions representing the curvilinear boundaries. Following Johns *et al.* [7], a spatial coordinate transformation rendered the physical domain into a rectangular one, and the shape of each island also became rectangular in the transformed domain. Boundary-fitted grid techniques for coastal and estuarine dynamics have been developed for many regions [15–19]. Johnson [15] employed an elliptic grid generation technique to study the vertically averaged riverine circulation where non-orthogonal boundary-fitted curvilinear grids for the physical domain were generated. Spaulding [16] developed a vertically integrated circulation model using boundary-fitted coordinates to simulate the  $M_2$  tide in the North Sea. Sheng [17] developed a boundary-fitted grid technique in a three-dimensional model for Chesapeake Bay and James River. Androsov *et al.* [18] used boundary-fitted curvilinear mesh in a 2D model for the Barents Sea, and Bao *et al.* [19] developed a 3D tidal model using boundary-fitted curvilinear grids for the Bohai Sea. Previous boundary-fitted transformed coordinate models developed for the head of the Bay of Bengal represented two opposite boundaries of the physical domain as straight lines along the open sea [5–11, 13].

In this article, the complete boundary surrounding the physical domain is represented by four boundary-fitted curves defined by four functions, and the four boundaries of each island are then represented approximately by two general functions. Appropriate transformations of the spatial coordinates render a square physical domain where the boundaries of each island are identifiable in the transformed domain. The vertically integrated shallow water equations are transformed into the new domain, and a regular explicit finite difference scheme is used to solve the shallow water equations. The model is applied to compute the water levels due to the tide and surges associated with some tropical storms that hit the coast of Bangladesh. Boundary-fitted grids are discussed in Section 2, the coordinate transformation adopted in Section 3, and the treatment of islands in Section 4. The model is presented in Section 5 and the finite difference scheme in Section 6, followed by a discussion of the results in Section 7 and a brief conclusion.

## 2. Boundary-Fitted Grids

It is natural to use Cartesian grids for flow within a rectangular or a square domain, and cylindrical or spherical grids for cylindrical or spherical grids, respectively. It is possible to generate conformal or orthogonal grids for relatively simple geometry, but for most estuarine and coastal applications the coastal geometry is usually quite complex so that conformal or orthogonal grids may not be suitable. Conventionally, non-orthogonal grids

for estuarine and coastal applications have been generated by solving partial differential equations — e.g. Sheng [17] employed Poisson equations, and Bao *et al.* [19] used an elliptic coordinate transformation equation satisfying some characteristics of curvilinear grids via a variational method. In this article, we use general curvilinear or boundary-fitted non-orthogonal grids to represent the model boundaries accurately in the numerical scheme, but they are generated in a different way. Our approach is based on the idea of Johns *et al.* [7], who represented the curvilinear boundary of the East Coast of India by a function, and on the idea of Roy [13] in representing the islands by a general function.

A rectangular Cartesian coordinate system is used, where the origin  $O$  is on the undisturbed level of sea surface — with  $Ox$  pointing towards the south,  $Oy$  towards the east, and  $Oz$  directed vertically upwards. Following Johns *et al.* [7], the northern coastal boundary that includes the coast of Bangladesh is given by  $x = b_1(y)$ , and the southern open sea boundary is given by  $x = b_2(y)$ . The western and eastern coastal boundaries are at  $y = d_1(x)$  and  $y = d_2(x)$ , respectively. This configuration is illustrated in Fig. 1, where the southern boundary  $x = b_2(y)$  is shown as a straight line but it may be a curve. It is also notable that the functions are not defined by explicit expressions, but in tabular form. Following Roy [13], the boundary-fitted grids are generated through the following general functions:

- the system of gridlines along  $x = b_1(y)$  and  $x = b_2(y)$  are given by

$$x = \{(m - q)b_1(y) + qb_2(y)\}/m, \quad (2.1)$$

where  $m$  and  $q$  are constants and  $0 \leq q \leq m$ ; and

- the system of gridlines along  $y = d_1(x)$  and  $y = d_2(x)$  are given by

$$y = \{(l - p)d_1(x) + pd_2(x)\}/l, \quad (2.2)$$

where  $l$  and  $p$  are constants and  $0 \leq p \leq l$ .

We note that Eq. (2.1) reduces to  $x = b_1(y)$  and  $x = b_2(y)$  for  $q = 0$  and  $q = m$ , respectively. Similarly, Eq. (2.2) reduces to  $y = d_1(x)$  and  $y = d_2(x)$  for  $p = 0$  and  $p = l$ , respectively. A suitable choice of  $\{q, m\}$  and  $\{p, l\}$  then appropriately generates the boundary-fitted curvilinear grid lines.

### 3. Coordinate Transformation

To facilitate the numerical treatment of an irregular boundary, we introduce the coordinate transformation where the new independent variables  $\xi$  and  $\eta$  are given by

$$\xi = \frac{x - b_1(y)}{b(y)}, \quad b(y) = b_2(y) - b_1(y), \quad (3.1)$$

$$\eta = \frac{y - d_1(x)}{d(x)}, \quad d(x) = d_2(x) - d_1(x). \quad (3.2)$$

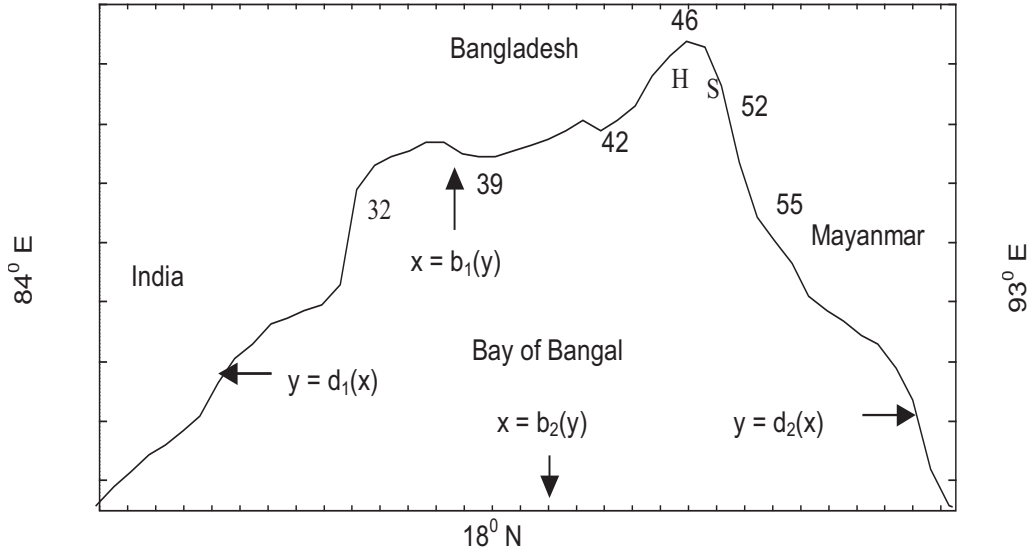


Figure 1: Boundaries of the analysis area and the locations at which results are presented. The locations are: 32 = Hiron Point, 39 = Barishal, 42 = Bhola, 46 = Char Jabbar (Noakhali), 44 = Hatiya (H), 50 = Sandwip (S), 52 = Chittagong and 55 = Cox's Bazar.

which map the physical curvilinear domain into the rectangular domain  $0 \leq \xi \leq 1$ ,  $0 \leq \eta \leq 1$  as the general functions given by (2.1) and (2.2) transform to

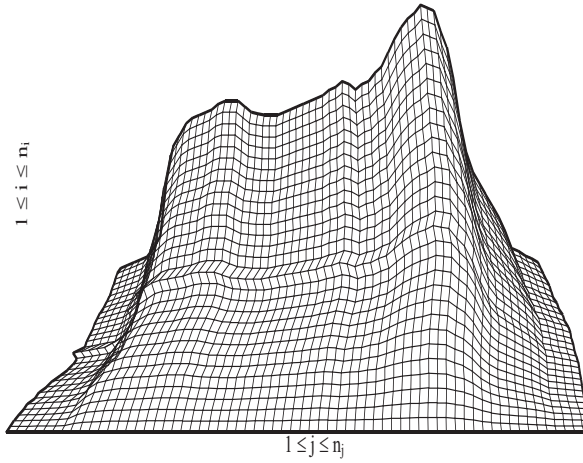
$$\xi = q/m, \quad (3.3)$$

$$\eta = p/l. \quad (3.4)$$

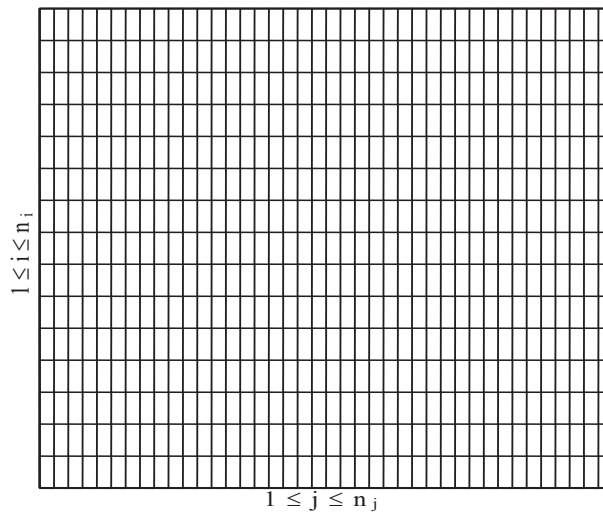
For  $q = 0$ , we have the coastal boundary  $x = b_1(y)$  or  $\xi = 0$ ; and for  $q = m$ , we have the open sea boundary  $x = b_2(y)$  or  $\xi = 1$ . Similarly, for  $p = 0$ , we have the western coastal boundary  $y = d_1(x)$  or  $\eta = 0$ ; and for  $p = l$ , we have the eastern coastal boundary  $y = d_2(x)$  or  $\eta = 1$ . Thus with an appropriate choice of the constants  $m$  and  $l$  and the parameters  $q$  and  $p$ , Eqs. (3.3) and (3.4) generate the rectangular grid system in the transformed domain. The curvilinear boundaries of a typical domain and the curvilinear grid system are shown in Fig. 2a, where one of the boundaries is a straight line but could be curved. The corresponding boundaries and the rectangular grid system following the transformation are shown in Fig. 2b.

#### 4. Representation of Islands

It is evident from the transformations (3.1) and (3.2) that the whereabouts of the boundaries of an island of arbitrary shape will be undetectable in the transformed domain unless the boundaries are aligned along the curvilinear grid lines defined by (2.1) and (2.2). Indeed, we cannot consider the actual shape of an island under the above transformation. Each of the northern and southern boundaries of an island is given by (2.1),



(a) Curvilinear boundaries and the curvilinear grid system.



(b) Boundaries and rectangular grid system in the transformed domain.

Figure 2: Curvilinear boundaries.

and each of the western and eastern boundaries is given by (2.2). After (3.1) and (3.2) are applied, the boundaries of the island are given by (3.3) and (3.4). Thus Eq. (3.3) with two different values of  $q$ , say  $q_1$  and  $q_2$  with  $q_1 < q_2$ , expresses the northern and southern boundary of an island. Similarly, Eq. (3.4) with two different values of  $p$ , say  $p_1$  and  $p_2$  with  $p_1 < p_2$ , expresses the western and eastern boundary of the island. The transformed

boundaries of an island are consequently

$$\xi = \frac{q_1}{m}, \quad \xi = \frac{q_2}{m}, \quad \eta = \frac{p_1}{l}, \quad \eta = \frac{p_2}{l}. \quad (4.1)$$

## 5. Mathematical Formulation

### 5.1. Vertically integrated shallow water equations

The rectangular Cartesian coordinate system was defined in Section 2. Relative to this coordinate frame, let the displaced position of the sea surface and the position of the sea floor be denoted by  $z = \zeta(x, y, t)$  and  $z = -h(x, y)$ , respectively. The vertically integrated shallow water equations adopted from Ref. [13] are

$$\frac{\partial \zeta}{\partial t} + \frac{\partial}{\partial x} \{(\zeta + h)u\} + \frac{\partial}{\partial y} \{(\zeta + h)v\} = 0, \quad (5.1)$$

$$\frac{\partial u}{\partial t} + u \frac{\partial u}{\partial x} + v \frac{\partial u}{\partial y} - f v = -g \frac{\partial \zeta}{\partial x} + \frac{\tau_x}{\{\rho(\zeta + h)\}} - \frac{c_f u (u^2 + v^2)^{1/2}}{(\zeta + h)}, \quad (5.2)$$

$$\frac{\partial v}{\partial t} + u \frac{\partial v}{\partial x} + v \frac{\partial v}{\partial y} + f u = -g \frac{\partial \zeta}{\partial y} + \frac{\tau_y}{\{\rho(\zeta + h)\}} - \frac{c_f v (u^2 + v^2)^{1/2}}{(\zeta + h)}, \quad (5.3)$$

where  $(u, v)$  are the components of the vertically integrated Reynolds averaged velocity,  $C_f$  is the friction coefficient and  $f$  is the Coriolis parameter.

The wind field over the physical domain is derived from an empirical formula [14], in which the sustained circulatory wind velocity measured at the radial distance  $r$  is

$$V_a(r) = \begin{cases} V_o(r/R)^{3/2}, & r \leq R, \\ V_o(R/r)^{1/2}, & r > R, \end{cases} \quad (5.4)$$

where  $V_o$  is the maximum value at the radial distance  $R$  from the eye of the storm. The radial and tangential components of the wind stress are given by

$$(\tau_r, \tau_\theta) = C_D \rho_a (u_a^2 + v_a^2)^{1/2} (u_a, v_a), \quad (5.5)$$

from which the respective  $x$  and  $y$  components  $\tau_x$  and  $\tau_y$  of the wind stress in (5.2) and (5.3) are derived from  $\tau_r$  and  $\tau_\theta$ . Here  $C_D$  and  $\rho_a$  are the drag coefficient and the density of air, respectively.

## 5.2. The boundary conditions

Following Johns *et al.* [9], the boundary conditions used are

$$u - v \frac{d}{dy}(b_1) = 0 \quad \text{at } x = b_1(y), \quad (5.6)$$

$$u - v \frac{d}{dy}(b_2) = (g/h)^{1/2} \zeta \quad \text{at } x = b_2(y), \quad (5.7a)$$

$$v - u \frac{d}{dx}(d_1) = 0 \quad \text{at } y = d_1(x), \quad (5.8)$$

$$v - u \frac{d}{dx}(d_2) = 0 \quad \text{at } y = d_2(x). \quad (5.9)$$

In generating the tide in the basin, the southern open sea boundary condition is taken to be

$$u - v \frac{d}{dy}(b_2) = (g/h)^{1/2} \zeta - 2(g/h)^{1/2} a \sin[(2\pi t)/T + \varphi] \quad \text{at } x = b_2(y), \quad (5.7b)$$

where  $a$  and  $\varphi$  denote the respective prescribed amplitude and phase of the tidal force and  $T$  is the tidal period.

## 5.3. Equations and boundary conditions in the transformed domain

From the transformation given by Eqs. (3.1) and (3.2), we have

$$\begin{aligned} \frac{\partial}{\partial x} &\equiv \frac{\partial \xi}{\partial x} \frac{\partial}{\partial \xi} + \frac{\partial \eta}{\partial x} \frac{\partial}{\partial \eta}, \\ \frac{\partial}{\partial y} &\equiv \frac{\partial \xi}{\partial y} \frac{\partial}{\partial \xi} + \frac{\partial \eta}{\partial y} \frac{\partial}{\partial \eta}, \end{aligned}$$

so Eqs. (5.1)-(5.3) transform to

$$\frac{\partial \zeta}{\partial t} + \frac{\partial}{\partial \xi} \{(\zeta + h)U\} + \frac{\partial}{\partial \eta} \{(\zeta + h)V\} = 0, \quad (5.10)$$

$$\begin{aligned} \frac{\partial u}{\partial t} + U \frac{\partial u}{\partial \xi} + V \frac{\partial u}{\partial \eta} - f v \\ = -g \left[ \frac{\partial \zeta}{\partial \xi} \frac{1}{b} - \frac{\partial \zeta}{\partial \eta} \frac{\{(d_1)_x + \eta d_x\}}{d} \right] + \frac{\tau_x}{\rho(\zeta + h)} - \frac{c_f u (u^2 + v^2)^{1/2}}{\zeta + h}, \end{aligned} \quad (5.11)$$

$$\begin{aligned} \frac{\partial v}{\partial t} + U \frac{\partial v}{\partial \xi} + V \frac{\partial v}{\partial \eta} + f u \\ = -g \left[ \frac{\partial \zeta}{\partial \eta} \frac{1}{d} - \frac{\partial \zeta}{\partial \xi} \frac{\{(b_1)_y + \xi b_y\}}{b} \right] + \frac{\tau_y}{\rho(\zeta + h)} - \frac{c_f v (u^2 + v^2)^{1/2}}{\zeta + h}, \end{aligned} \quad (5.12)$$

where

$$U = u \frac{\partial \xi}{\partial x} + v \frac{\partial \xi}{\partial y} = \frac{u - \{(b_1)_y + \xi b_y\}v}{b}, \quad (5.13)$$

$$V = u \frac{\partial \eta}{\partial x} + v \frac{\partial \eta}{\partial y} = \frac{v - \{(d_1)_x + \eta d_x\}u}{d}. \quad (5.14)$$

The boundary conditions Eqs. (5.6)-(5.9) transform to

$$U = 0 \quad \text{at } \xi = 0, \quad (5.15)$$

$$bU - (g/h)^{1/2}\zeta = 0 \quad \text{at } \xi = 1, \quad (5.16a)$$

$$bU - (g/h)^{1/2}\zeta = -2(g/h)^{1/2}a \sin [(2\pi t)/T + \varphi] \quad \text{at } \xi = 1, \quad (5.16b)$$

$$V = 0 \quad \text{at } \eta = 0, \quad (5.17)$$

$$V = 0 \quad \text{at } \eta = 1. \quad (5.18)$$

At each boundary of an island the normal component of velocity vanishes, so from (4.1) the boundary conditions for an island are

$$U = 0 \quad \text{at } \xi = \frac{q_1}{m} \quad \& \quad \xi = \frac{q_2}{m}, \quad (5.19)$$

$$V = 0 \quad \text{at } \eta = \frac{p_1}{l} \quad \& \quad \eta = \frac{p_2}{l}. \quad (5.20)$$

## 6. Finite Difference Scheme

In the physical domain, the curvilinear grid system is generated through Eqs. (2.1) and (2.2); and in the transformed domain, the corresponding rectangular grid system is generated through Eqs. (3.3) and (3.4) with an appropriate choice of  $m$ ,  $l$ ,  $q$ , and  $p$ . Discrete coordinate points in the transformed domain at the respective grid widths  $\Delta\xi$  and  $\Delta\eta$  are defined by

$$\begin{aligned} \xi &= \xi_i = (i-1)\Delta\xi, & i &= 1, 2, \dots, n_i, \\ \eta &= \eta_j = (j-1)\Delta\eta, & j &= 1, 2, \dots, n_j, \end{aligned}$$

and the sequence of times using the time step  $\Delta t$  are

$$t = t_k = k\Delta t, \quad k = 1, 2, 3, \dots$$

A staggered grid is appropriate, in which there are three distinct types of computational point. When  $i$  and  $j$  are both even, the point is a  $\zeta$ -point at which  $\zeta$  is computed; if  $i$  is odd and  $j$  is even, the point is a  $u$ -point at which  $u$  is computed; and if  $i$  is even and  $j$  is odd, the point is a  $v$ -point at which  $v$  is computed. We choose  $n_i (= 30)$  to be even, so that at the southern open boundary there are  $\zeta$ -points and  $v$ -points only. Similarly, we choose  $n_j (=$

65) to be odd, ensuring there are only  $\zeta$ -points and  $\nu$ -points at the eastern and western boundaries. The coastal boundary is approximated either along the nearest odd grid line ( $i = \text{odd}$ ) given by Eq. (2.1) when there are only  $u$ -points on this part of the boundary, or along the nearest odd grid line ( $j = \text{odd}$ ) given by Eq. (2.2) so there are only  $\nu$ -points along that part of the boundary. The island boundaries are approximated in the same manner. The boundaries of the coast and of the islands are thus represented by a system of stair steps, such that at each segment (stair) there exists only the velocity component normal to the segment, ensuring the normal component of velocity vanishes at the boundaries in the numerical scheme. The governing equations (5.10)-(5.12) and the boundary conditions (5.15)-(5.18) are discretised by finite differences forward in time and central in space, and are solved by a conditionally stable semi-implicit method using the staggered grid. For numerical stability, the velocity components in Eqs. (5.11) and (5.12) are modelled in a semi-implicit manner. For example, in the last term of Eq. (5.11) the time discretisation of  $u(u^2 + v^2)$  is rendered  $u^{k+1}(u^2 + v^2)^k$ , where the superscript  $k$  and  $k + 1$  denote values at the present and advanced time levels, respectively. Moreover, the CFL criterion was satisfied in order to ensure the stability of the numerical scheme, with the time step of  $\Delta t = 120$  seconds adopted. Along the closed boundary, the zero normal component of the velocity is easily achieved through an appropriate stair step representation as already mentioned. The initial values of  $\zeta$ ,  $u$ , and  $\nu$  are set to zero.

## 7. Results and Discussion

### 7.1. Analysis of the computed surge response

As foreshadowed, the model was applied to compute the water levels due to both tides and surges associated with tropical storms that hit the coast of Bangladesh. The area considered extends from  $84^\circ\text{E}$  to  $96^\circ\text{E}$  along the coast of Bangladesh, India and Myanmar (Burma). The open sea boundary is situated along  $18^\circ\text{N}$  (Fig. 1). The east-west extent varies between  $734 \text{ km}$  and  $1035 \text{ km}$ , and the north-south extent varies between  $208 \text{ km}$  and  $541 \text{ km}$ . The relevant area was divided into  $30 \times 65$  grid points, so that in the north-south direction  $\Delta x$  varied between  $7.17 \text{ km}$  and  $18.65 \text{ km}$ , while in the east-west direction  $\Delta y$  varied between  $11.47 \text{ km}$  and  $16.17 \text{ km}$ . In the transformed domain, we set  $m = l = 1.0$ ; and for uniform mesh we considered  $\Delta \xi = 1.0/(n_i - 1)$ , and  $\Delta \eta = 1.0/(n_j - 1)$ , such that  $q_i = (i - 1)\Delta \xi = \xi_i$  and  $p_j = (j - 1)\Delta \eta = \eta_j$ . As mentioned, the offshore region of Bangladesh coast has many large and small islands, with a high density around the Meghna estuary. It is possible to incorporate the small islands by considering a very fine resolution in the numerical scheme, but there are some practical problems in doing so — viz. instability of the numerical scheme, more computing time, and a high memory requirement etc. Since a very high resolution was not ensured in the simulation, only two major islands were included — viz. Sandwip and Hatiya. The largest island Bhola is located very near to the coastline, so it was considered to be part of the mainland — cf. Fig. 1.

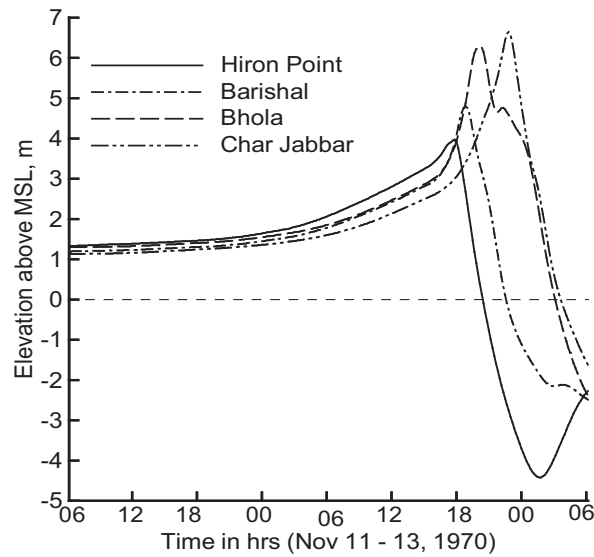
The storms of November 1970, December 1981 and May 1985 were considered, with

Table 1: History of the chosen storms.

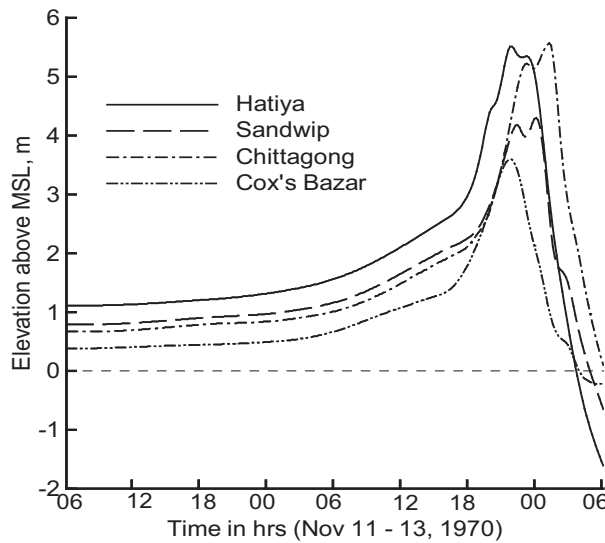
Storm of November 1970				Storm of December 1981				Storm of May 1985			
Date	Hour	Lat.	Long.	Date	Hour	Lat.	Long.	Date	Hour	Lat.	Long.
09	2200	14.10	86.00	08	0100	13.30	85.25	22	0000	14.00	88.50
10	0600	14.50	86.00	08	0600	14.00	86.00	22	0600	14.50	88.20
10	1800	16.00	86.00	08	0900	14.50	86.20	22	1800	15.50	87.50
11	1800	17.50	86.00	09	0600	16.00	87.00	23	0600	16.00	87.50
12	0600	19.00	87.50	09	1800	17.50	87.00	23	1200	17.00	87.50
12	1500	20.00	88.50	10	0000	18.50	88.00	23	1800	17.50	87.50
12	1800	21.50	90.00	10	0900	19.50	88.50	24	0900	18.00	88.00
13	0600	23.25	93.00	10	1500	20.00	88.50	24	1500	19.50	89.00
				10	2100	21.00	89.00	24	2100	20.50	90.50
				11	0300	21.80	89.50	25	0200	21.50	91.50
				11	0900	22.75	90.00	25	0800	23.50	92.50

respective maximum sustained anticlockwise circulatory wind velocities of 62 m/s, 36 m/s and 42 m/s. Table 1 gives the history of these storms, with data from the Bangladesh Meteorological Department (BMD). The storm of 1970 was one of the most severe of the twentieth century to hit the coast of Bangladesh, and featured a high surge due to both wind intensity and the path it followed [12], so more emphasis is placed on the 1970 storm data for the computation. Two types of ocean depth topography were considered — viz. a uniform depth of 15 m, and a representative variable depth. Uniform values of 0.0026 for the friction coefficient ( $C_f$ ) and 0.0028 for the drag coefficient ( $C_D$ ) were assumed throughout the physical domain.

The storm of November 1970 moved approximately northward and on 12 November it gradually turned and crossed the coast (landfall) of Bangladesh near Chittagong (location 52) in the early morning (at approximately 0030 hrs) of 13 November — cf. Table 1. Figs. 3a and 3b depict the computed time series of the surge levels associated with this storm at different coastal locations, for the representative variable depth bathymetry. The water level at each location increases with time as the storm approaches the coast and then recedes. At Hiron Point a strong recession occurs after 1700 hrs of November 12, earlier than in any other location and about 7.5 hrs before landfall of the storm (Fig. 3a). The recession is due to the backwash of water from the shore towards the sea. Hiron Point is situated far west of the storm path, so the direction of the anticlockwise circulatory wind becomes southerly (i.e. towards the sea) at Hiron Point long before the storm reaches the coast, driving the water towards the sea. The recession peaks at up to  $-4.5$  metres at 0100 hrs on 13 November. It may be noticed that the recession at Barisal, Bhola, and Char Jabbar begins at approximately at 1900, 2000 and 2300 hours, respectively (Fig. 3a). Thus the beginning of the recession is delayed towards the east as expected. At every location except Chittagong, the peak surge is attained before the landfall time of the storm



(a) Hiron Point (32), Barisal (39), Bhola (42), and Char Jabbar (46)



(b) Hatiya (44), Sandwip (50), Chittagong (52), and Cox's Bazar (55)

Figure 3: Computed time series of surge levels at coastal locations for the November 1970 storm.

as expected, since the circulatory wind intensity is highest along the coast when the storm nears the coast. The maximum elevation varies between 3.75 metres (at Cox's Bazar, 55) to 6.5 metres (at Char Jabbar, 46). At Chittagong (52), the computed water level increases

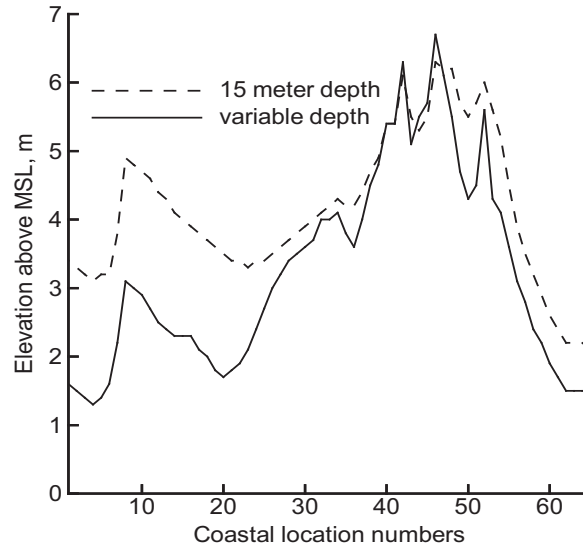


Figure 4: Computed maximum surge levels at different locations along the coastal belt for the November 1970 storm, assuming two different types of bathymetry.

up to 5.5 metres before the recession starts after 0100 of November 13, approximately half an hour after landfall (Fig. 3b). Since the storm crosses the coast just north of Chittagong at approximately 0030 hrs, the wind over Chittagong to the right of the path must be very strong even after landfall, which may be responsible for the peak elevation at 0100 hrs. The water level is also computed to see the response of the model for uniform depth. It is qualitatively similar to that computed for representative variable bathymetry, and increases for smaller uniform depths (not shown) because the amplitude of the long wave increases in shallow water. Fig. 4 shows the computed peak surge values at the coastal locations for representative bathymetry and for uniform depth of 15 metres. It may be observed that the coastal region between Barisal and Chittagong is vulnerable to very high surge. For a 15 metre uniform bathymetry, the computed peak water levels show an overall increase over those with variable bathymetry, but the two relevant curves shown in Fig. 4 are qualitatively similar.

## 7.2. Analysis of the computed tide and surge superposition

As mentioned, the shallow water model is designed for computing both tides and surges, and their nonlinear interaction. The purely tidal oscillation is the initial dynamical condition for the interaction, but the main difficulty in generating the tidal oscillation in the model simulation process lies with its amplitude and phase. In the actual basin, different tidal components mutually interact, so there are diurnal inequalities and non-periodic oscillation. Moreover, there is also variation of the tidal amplitude in the spring-neap cycle. The complexity of tidal phenomena is a major constraint in generating actual tidal

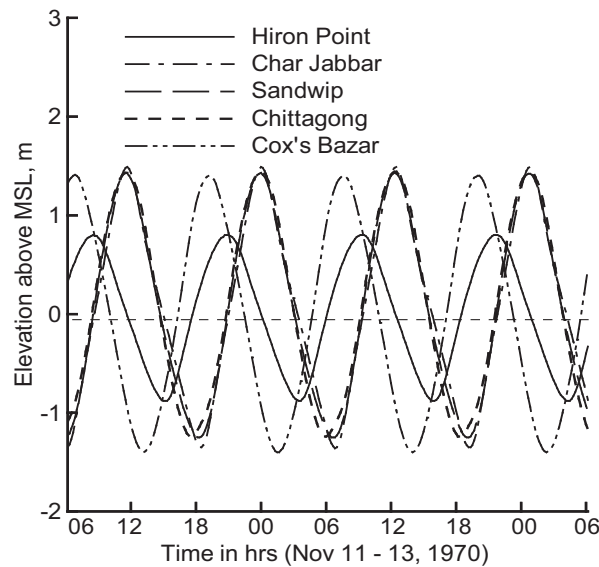


Figure 5: Computed tidal oscillation at different coastal locations.

oscillation in the simulation. The actual tidal oscillation also has to be generated for each storm period, which is always difficult and time consuming. Thus the dynamical interaction of tide and surge may not always be feasible. An alternative way to incorporate tidal oscillations with surges is to superimpose the time series of surge responses at each location obtained through model simulation with the tidal oscillation at that location obtained from tide tables. Tidal high and low values at different locations is generally available, four times a day in the Bangladesh Tide Table. The time series of tidal oscillation at each location may therefore be generated using cubic spline interpolation.

The tide is generated in the model through the south open boundary condition (5.16b), for suitable values of  $a$ ,  $T$  and  $\varphi$  in the absence of wind stress. Although there is variation in the tidal period at the head of the Bay of Bengal, the average period is approximately that of the  $M_2$  astronomical tide so that  $T = 12.4$  hrs was assumed, and it was found that  $\varphi = 0$  is a good choice for the region. Data on the amplitude  $a$  along the southern boundary was not available, but  $a = 0.6$  metres was chosen to test the response of the model along the coastal belt (Fig. 5). The response was found to be exactly sinusoidal with the same period 12.4 hours, as expected. The computed amplitude is almost same (approximately 1.4 metres) everywhere, except at Hiron Point. However, according to the Bangladesh Tide Table the tidal amplitude is highest (nearly 1.75 metres) in the Meghna estuary (e.g. at Sandwip and Char Jabbar), and at Cox's Bazar it is approximately 1.0 metre. A uniform value of  $a = 0.6$  metres was adopted everywhere on the south boundary (5.16b), which may not be suitable. Thus with a more appropriate choice for the amplitude  $a$ , the actual tidal oscillation may be better reproduced at each location. For the phase of the tidal oscillation, it may be seen that Char Jabbar, Sandwip and Chittagong are in the same phase

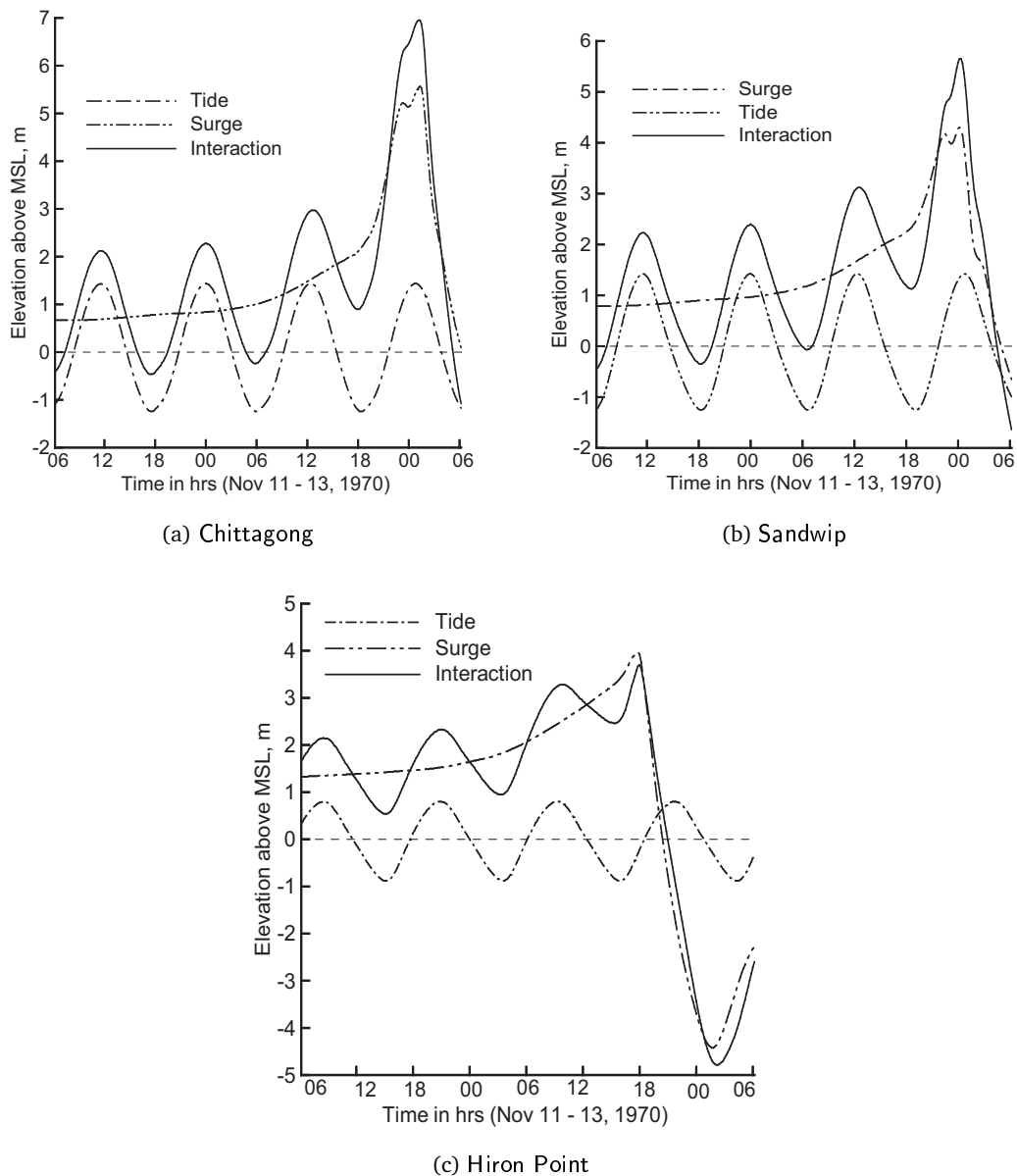


Figure 6: Time series of the water level due to the tide, surge and their interaction during the November 1970 storm.

— and they are very close locations. Consequently, appropriate values of the amplitude  $a$  along the southern open sea boundary condition in the model may generate the actual tidal oscillation in the whole basin. Further investigation on appropriately generating actual tidal oscillations is in progress.

Fig. 6 shows the tide (dash-dot line), computed surge (dash-dot-dot line), and the lin-

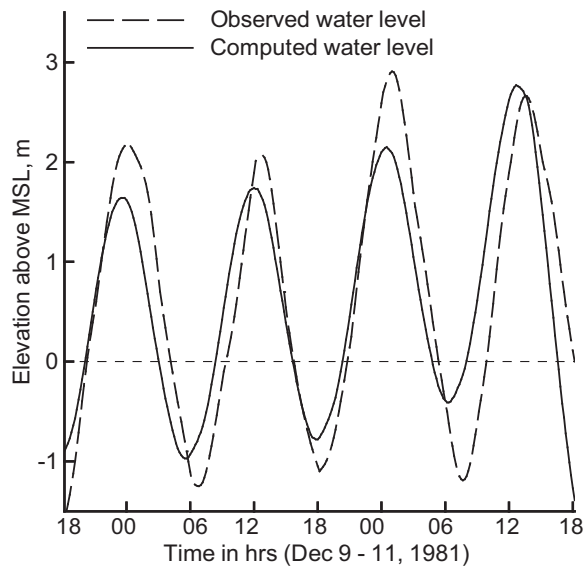
ear interaction (tide and surge, solid line) associated with the November 1970 storm at Chittagong, Sandwip and Hiron Point. The maximum water levels at Chittagong due to tide, surge and their interaction are 1.45, 5.5 and 6.95 metres, respectively — (Fig. 6a). According to the Bangladesh Meteorological Department, the estimated water level at Chittagong is 6 to 9 metres, so the computed water level is within this range. The storm approaches the coast during high tide period at Chittagong, and hence intensifies the water level due to interaction. An almost similar feature is seen at Sandwip (Fig. 6b), very near to Chittagong. On the other hand, the peak surge at Hiron Point coincides with zero tidal amplitude, so the total water level is not as high (Fig. 6c). The sharp fall of the curve indicates the strong recession at Hiron Point discussed earlier. At each location, the surge response is less when the storm is away from the coast as the wind is then relatively weak, and the total water level is dominated by tidal oscillation. On the other hand, due to the very strong wind when the storm nears the coast the water level is then dominated by surge.

### 7.3. Comparison between computed and observed time series of water levels

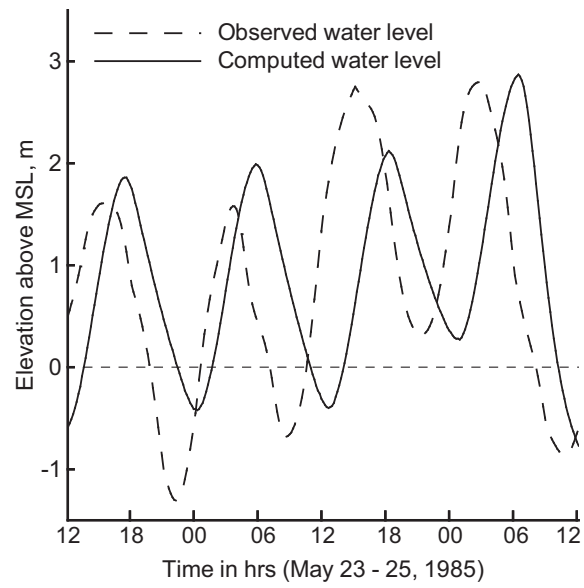
The validation of a model depends upon correct observational data, but authentic time series of observed water level data are very limited. The Hydrographic Department of the Bangladesh Inland Water Transport Authority collects water level data at different coastal locations through manual gauge readers, but during a severe storm period it is not possible for observers to stay in the gauge station to collect data, so water level data for severe storm periods are usually unavailable. However, some data were collected [12] and used here. Fig. 7 depicts the computed water levels (tide and surge) and observed water levels at Chittagong for the 1981 storm and at Hatiya for the 1985 storm. At Chittagong, the computed water level is seen to be less than that actually observed, except in the final peak at 1200 hrs of 11 December (Fig. 7a). Indeed, it was not possible to choose the tidal oscillation for the purpose of interaction. At Hatiya, there is satisfactory agreement in the amplitude despite the difference in phase (Fig. 7b). Thus although the computation could be improved by a better representation of the tidal oscillation, the agreement between the computed and observed water levels is fairly satisfactory.

The results in Fig. 8 depict the maximum surge levels at different coastal locations due to the 1970 storm, in the presence and absence of islands. The computed results show that the surge level decreases in the presence of islands. It is also found that the region between Barishal (location 39) and Cox's Bazar (location 55) is vulnerable to high surge, in agreement with observation.

The sensitivity of the surge level with respect to the intensity of a storm was also tested. Fig. 9 shows the peak surges along the coastal locations due to the storms of 1970, 1981 and 1985, with circulatory wind velocities 62, 36 and 42 metres per second, respectively. The surge due to the November 1970 storm is found to be much higher, not only due to it possessing the strongest wind but also because of its path [12]. Although the wind velocity is less for the 1981 storm at locations between 25 and 40, its surge level is higher than for the 1985 storm, and this is attributed to their respective paths — cf. Table 1.



(a) 1981 storm at Chittagong



(b) 1985 storm at Hatiya

Figure 7: Computed and observed water levels.

The contours at the time of landfall of the storm in Fig. 10a show a positive surge in the eastern region and recession in the western part of the domain, as mentioned earlier.

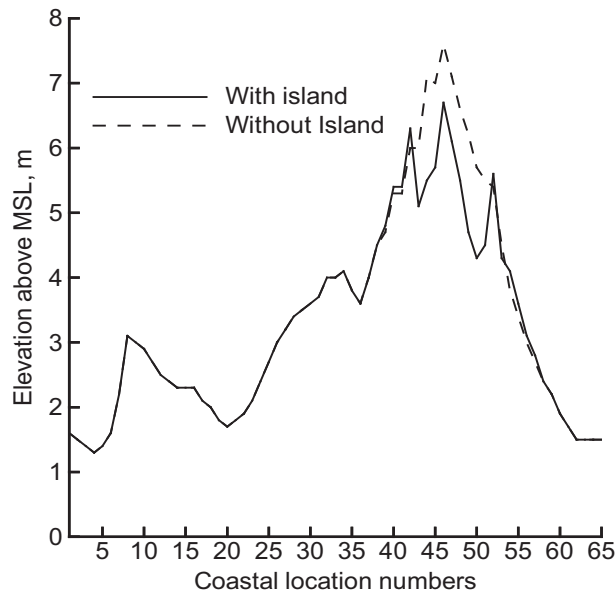


Figure 8: Computed peak surge levels associated with November 1970 storm, in the presence and absence of the offshore islands.

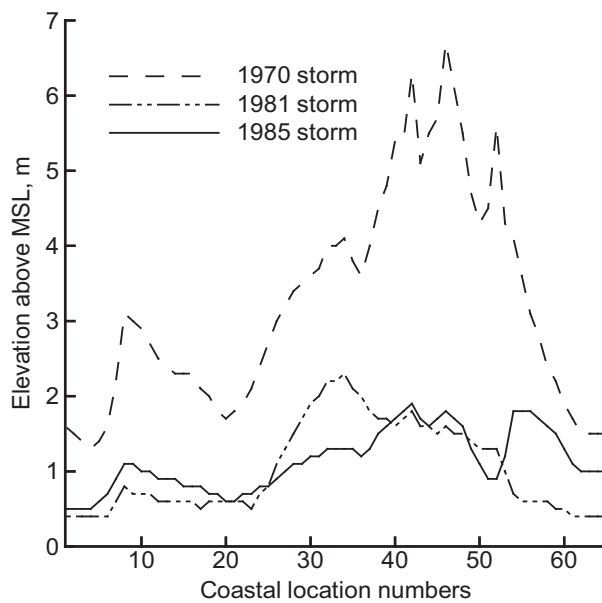
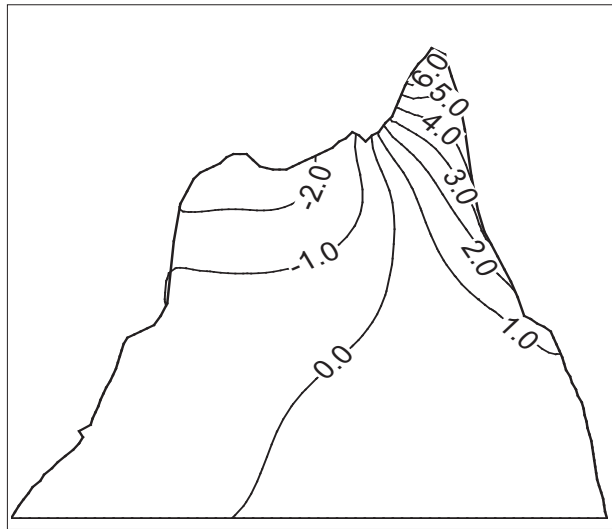
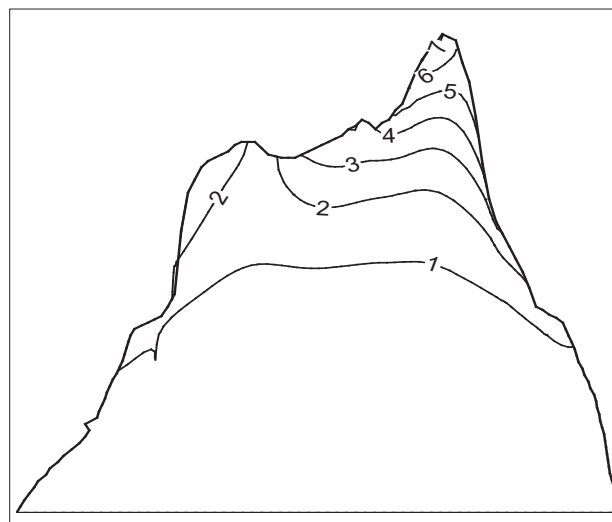


Figure 9: Computed peak surge levels associated with 1970, 1981, and 1985 storms.

Fig. 10b depicts the contours (in metres) for the maximum surge levels in the whole domain associated with the 1970 storm. The water level is 7 metres along the coastal belt



(a) surface elevation for surge levels along the coastal region of Bangladesh at the time of landfall



(b) surface elevation for peak surge levels along the coastal region of Bangladesh

Figure 10: Contours (in meters) of equal sea associated with 1970 storm.

between Char Jabbar and Chittagong, and surge levels in the west are less than those in the east. One reason for this is that the west is to the left of the storm path, and another reason is that the eastern region is shallower than the western region (surge amplitude increases in shallow water).

## 8. Conclusion

The implemented shallow water model proved quite capable of producing results on both tide and surge in the head of the Bay of Bengal. Oceanographic, meteorological and geographic data was used to ensure accuracy. The model may be applied to compute water levels along the East Coast of India and the coast of Burma — and may also be applicable in any bay or estuary, or even in confined lakes.

## Acknowledgments

The mathematical formulation in this paper was carried out under the supervision of Professor G. D. Roy, the great Bangladeshi scientist and researcher in the field of Dynamic Meteorology who died on 25<sup>th</sup> December, 2008. The author dedicates this article to him, in recognition of her gratitude and deep respect.

## References

- [1] Das, P. K. (1972) Prediction model for storm surges in the Bay of Bengal. *Nature* **239**, 211–213.
- [2] Flierl, G. R. and Robinson, A. R. (1972) Deadly surges in the Bay of Bengal: Dynamics and storm tide tables. *Nature* **239**, 213–215.
- [3] Das, P. K., Sinha, M. C. and Balasubrahmanyam, V. (1974) Storm surges in the Bay of Bengal. *Quart. J. Roy. Met. Soc.* **100**, 437–449.
- [4] Johns, B. and Ali, A. (1980) The numerical modeling of storm surges in the Bay of Bengal. *Quart. J. Roy. Met. Soc.* **106**, 1–18.
- [5] Dube, S. K., Sinha, P. C. and Roy, G. D. (1985) The numerical simulation of storm surges along the Bangladesh coast. *Dynam. Atmos. Oceans* **9**, 121–133.
- [6] Dube, S. K., Sinha, P. C. and Roy, G. D. (1986) The numerical simulation of storm surges in Bangladesh using a bay-river coupled model. *Coast Eng.* **10**, 85–101.
- [7] Johns, B., Dube, S. K., Mohanti, U. C. and Sinha, P. C. (1981) Numerical simulation of surge generated by the 1977 Andhra cyclone. *Quart. J. Roy. Soc. London* **107**, 919–934.
- [8] Johns, B., Dube, S. K., Mohanti, U. C. and Sinha, P. C. (1982) The simulation of continuously deforming lateral boundary in problems involving the shallow water equations. *Comput. Fluids* **10**, 105–116.
- [9] Johns, B., Rao, A. D., Dube, S. K. and Sinha, P. C. (1985) Numerical modeling of tide-surges interaction in the Bay of Bengal. *Phil. Trans. R. Soc. London A* **313**, 507–535.
- [10] Sinha, P. C., Dube, S. K. and Roy, G. D. (1986) Numerical simulation of storm surges in Bangladesh using a multi-level model. *Int. J. Num. Methods Fluids* **6**, 305–311.
- [11] Roy, G. D. (1985) Some aspects of storm surges along the coast of Bangladesh. *Ganith - J. Bangladesh Math. Soc.* **6**(1), 1–8.
- [12] Roy, G. D. (1995) Estimation of expected maximum possible water level along the Meghna estuary using a tide and surge interaction model. *Environ. Int.* **21**(5), 671–677.
- [13] Roy, G. D. (1999) Inclusion of offshore islands in transformed coordinates shallow water model along the coast of Bangladesh. *Environ. Int.* **25**(1), 67–74.
- [14] Jelesnianski, C. P. (1965) A numerical calculation of storm tides induced by a tropical storm impinging on a continental shelf. *Mon. Wea. Rev.* **93**, 343–358.

- [15] Johnson, B. H. (1982) Numerical modeling of estuarine hydrodynamics on a boundary fitted coordinate system. In *Numerical Grid Generation* (Thompson, J. ed.) Elsevier Science, 419–436.
- [16] Spaulding, M. L. (1984) A vertical averaged circulation model using boundary-fitted coordinates. *J. Phys. Oceanogr.* **14**, 973–982.
- [17] Sheng, Y. P. (1989) On modeling three-dimensional estuarine and marine hydrodynamics. In *Three-dimensional Models of Marine and Estuarine Dynamics* (Nihoul, J. C. J. and Jamart, B. M. ed.) Elsevier Oceanography, Series 45, 35–54.
- [18] Androsov, A. A., Vol'tzinger, N. E. and Liberman, Y. M. (1997) A two dimensional tidal model of the Barents Sea. *Oceanology* **37**, 16–22.
- [19] Bao, X. W., Yan, J. and Sun, W. X. (2000) A three-dimensional tidal model in boundary-fitted curvilinear grids. *Estuar. Coast. Shelf Sci.* **50**, 775–788.